Available online at www.eccomasproceedia.org
Eccomas Proceedia COMPDYN (2025) 2055-2067

ECCOMAS
Proceedia

COMPDYN 2025
10th ECCOMAS Thematic Conference on
Computational Methods in Structural Dynamics and Earthquake Engineering
M. Papadrakakis, M. Fragiadakis (eds.)
Rhodes Island, Greece, 15-18 June 2025

TENSILE BEHAVIOR OF LINEAR FASTENING SYSTEMS IN MASONRY STRUCTURES

Pietro Crespi[1], Manuela Scamardo[1], and Sara Cattaneo[1]

[1] Department of Architecture, Built Environment and Construction Engineering, Politecnico di Milano
Piazza Leonardo da Vinci 32, Milano, Italy
e-mail: name@e-mail.address
{pietro.crespi, manuela.scamardo, sara.cattaneo}@polimi.it

Abstract

The seismic retrofit of existing masonry structures often requires the improvement of the connection between the slabs and the walls of the building. Common interventions use post-installed bonded anchors in the shape of linear fastening systems to strengthen the wall-to-wall and roof-to-wall connections in order to achieve the box-like behavior of the structure.
Although this type of application is quite common, there is still a lack of knowledge about the tensile behavior of linear fastening systems because the most of the experimental results obtained in the assessment tests are limited to single or double anchor systems.
In order to overcome this problem, an experimental campaign was carried out on linear groups of one to five 12 mm threaded bars installed with an adhesive in solid brick masonry specimens. The experimental layout was defined to take into account the most critical configurations (i.e. installation in the mortar joint, limited embedment depth, small spacing) and a special device was designed to ensure a linear distribution of the applied displacements on the group of anchors.
The test results obtained are discussed and numerical simulations are presented to highlight the influence of the geometrical imperfections (i.e. eccentricity of the applied load with respect to the center of the group of anchors) as well as the scatter of the strength of the different anchors on the overall capacity of the linear fastening system.

Keywords: Masonry structures, seismic retrofitting, bonded anchors, linear fastening, slab-to-wall connections.

ISSN:2623-3347 Published by Eccomas Proceedia.
Peer-review under responsibility of the organizing committee of COMPDYN 2025.
doi: 10.7712/120125.12550.24811

1 INTRODUCTION

Unreinforced masonry structures have shown in the past to be highly vulnerable to earthquake loadings [1]. One of the main problems of these structures is the poor connection between orthogonal walls or between walls and floors. To overcome this problem, retrofitting interventions are often adopted to improve the connection between walls and horizontal diaphragms in order to obtain the so-called "box-like behavior" of the structure [2].

The use of multiple anchors in a uniformly spaced linear configuration is one of the most commonly used interventions to connect masonry walls. The mechanical behavior of single anchors under different installation and loading conditions has been extensively studied in the past [3–7]. More recently, some research has been developed on full scale wall-to-wall connections, including the effect of cyclic loading on both unreinforced and retrofitted configurations [8–11]. Furthermore, wall-to-timber connections have also been investigated [12,13].

Even if the linear distribution of anchors seems to be a very simple application, its design according to the European standard [14] is not so simple because the code only covers the case of two anchors, neglecting configurations involving multiple anchors.

The purpose of this paper is to investigate the behavior of uniformly spaced linear configurations of multiple bonded anchors, including up to five anchors, under tension loading. Anchors with different configurations were installed in the mortar joints, considering a critical ratio of spacing to embedment depth equal to 1.

The test results showed that the behavior of the anchor group can be influenced by the uniformity of the applied displacement, which can be related to the presence of a certain eccentricity between the load application point and the stiffness center of the anchor group. In order to better understand the influence of these parameters, a simple numerical model has been implemented considering different levels of eccentricity (0 to 5%) and different values of anchor failure load. The interaction between anchors, due to the small spacing, was also considered by analytical formulation. The results showed that the interaction between anchors is the most important contribution, which tends to be stable for more than 5 anchors.

2 EXPERIMENTAL CAMPAIGN

To investigate the relationship between the number of anchors in a group and the maximum load capacity of the linear fastening system, some tests were carried out on different sets of M12 threaded bars installed with adhesive in solid clay brick walls. Single anchors were tested first (reference tests), followed by groups of 2 to 5 anchors.

2.1 Materials and specimens

Four masonry walls of 129×129×25 cm with 2 wythes English bond layout were built in September 2022 (specimens W0, W1, W2) and in October 2023 (specimen W3). Solid clay "Rosso Vivo" bricks with dimensions 250×120×55 mm were used. The mean compressive [15] and splitting [16] strengths of the brick are 23.30 MPa and 2.46 MPa, respectively.

Mortar joints were made with masonry mortar classified as M2.5, with mean compressive [17] and bending [18] strengths of 4.80 MPa and 1.91 MPa, respectively, for specimens W0, W1, W2, and 3.96 MPa and 1.15 MPa, respectively, for specimen W3.

M12 threaded bars (steel grade 8.8 [19]) were installed in 14 mm pre-drilled holes with an embedment depth h_{ef} = 100 mm. A spacing s = 100 mm was assumed for the linear fastening system in order to test the worst configuration (spacing equal to the embedment depth, s/h_{ef} = 1).

All anchors were installed into the mortar joints using Hilti HIT-HY 270 [20] adhesive and tested at least 24 hours after curing.

2.2 Test plan and tested configurations

A total of 22 tension tests were performed on different anchor groups. The test coding adopted to identify the different tested configurations follows this rule: number of anchors (#A), embedment depth (in mm), external prestress applied to the wall (in MPa, see section 2.3), wall specimen (W#), progressive number of the test. The additional "*" is reported for those tests, where the loading protocol has been modified to impose a uniform displacement to all anchors (see section 2.3). Only reference tests on single anchors were executed on wall W0 since this specimen was previously used to perform other tests related to a different experimental campaign. Figure 1 shows a sketch of the four wall specimens with the installation position of the anchors of each test. Anchors were always installed into the mortar bed joints, possibly into (or close to) a T-joint (intersection of horizontal and vertical joints) to consider the worst installation conditions according to [21].

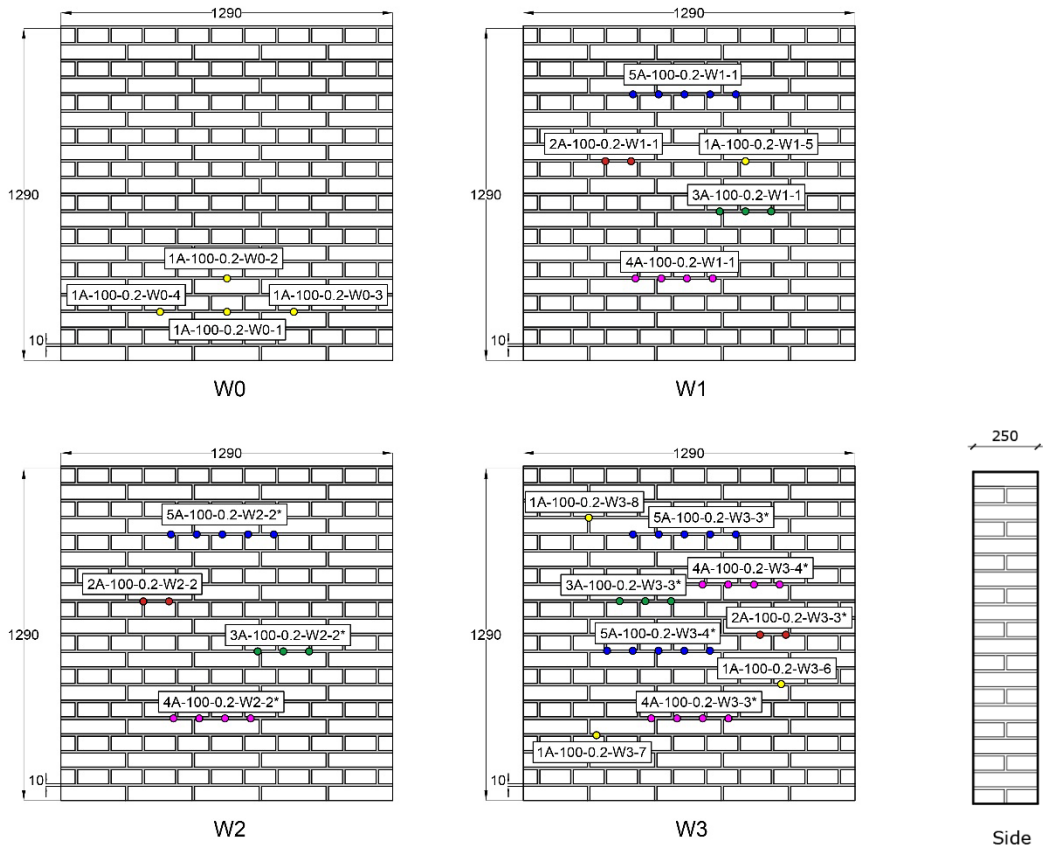

Figure 1: Sketch of masonry specimens with the position of the tested anchors.

2.3 Test setup

The tests were performed using three steel rigs. The first steel rig applied a uniform pressure of 0.20 MPa to prestress the wall specimen through a couple of Dywidag bars. The second steel frame was designed to fix the masonry wall to the ground by means of a couple of beams (grey beams in Figure 2, left) spaced 80 cm apart to ensure an unconfined configuration of the anchors and to prevent bending failure of the wall. Finally, the third steel frame applied the tensile load to the group of anchors and included a hydraulic jack with a capacity of 300 kN and a load cell.

The anchors were connected to the steel frame by a rigid baseplate (Figure 2, right). All tests were monitored with two LVDTs (Linear Variable Differential Transformers) placed at each end of the baseplate (Figure 2, right) and all data were recorded using the MOOG acquisition

system. The tensile tests were performed under displacement control at a constant rate of 0.015 mm/s.

During the tests, rotation of the baseplate sometimes occurred (Figure 3, left). This phenomenon, which has already been pointed out by other researchers [21], is due to the dispersion of the resistance of the anchors in a group and to a possible undesired eccentricity between the axis of the jack and the center of the baseplate. In order to verify the influence of this phenomenon on the load bearing capacity of the anchor group, some tests were executed with an anti-rotation system consisting of a pair of threaded control bars equipped with load cells that measure the contact reaction between the bar and the baseplate in case of rotation of the system (Figure 3, right). These rotation prevented tests are marked with "*" in Figure 1.

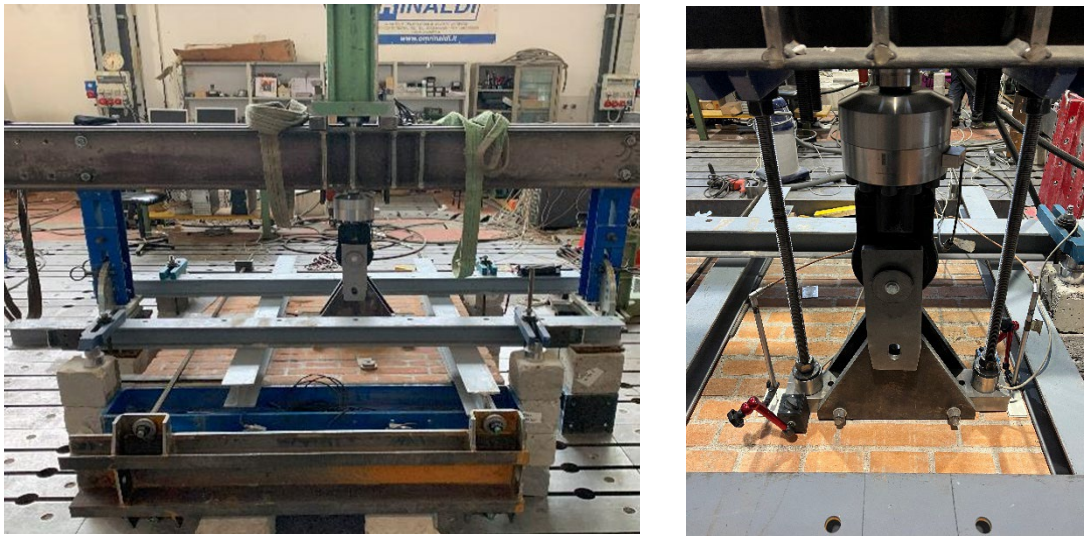

Figure 2: Test setup (left), rigid baseplate and LVDTs (right).

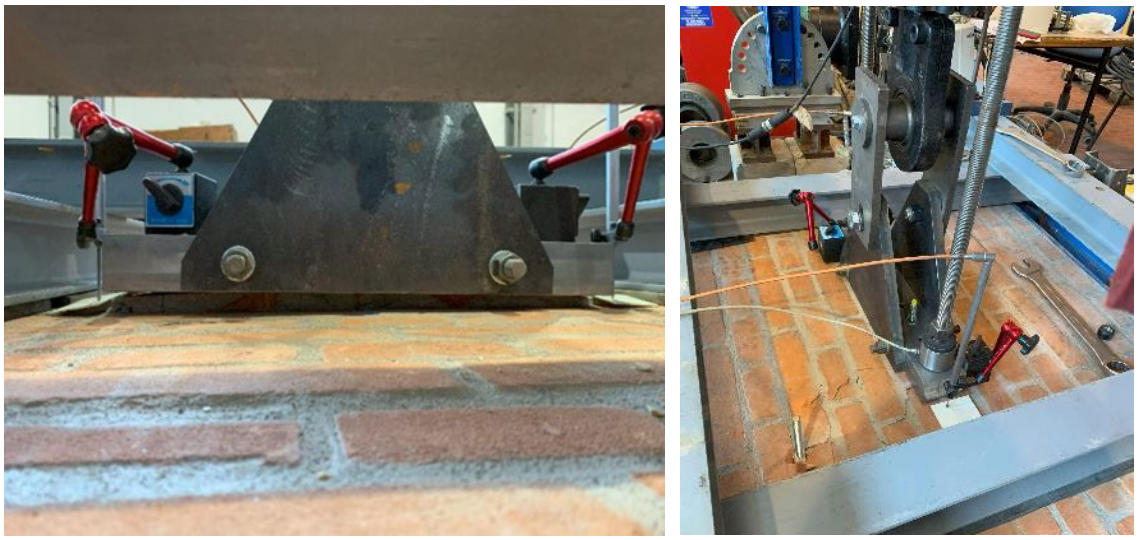

Figure 3: Baseplate rotation (left, test 3A-100-0.2-W1-1) and baseplate anti-rotation system (right).

3 TEST RESULTS

If the left and right displacements of the baseplate begin to differ during the test, the control bars are activated to control the rotation of the system and ensure a uniform distribution of the imposed displacements on the anchors. Activation of the control bar implies the appearance of

a compression load in it. This control load could change the value of the load acquired along the hydraulic jack. For this reason, Table 1 shows the maximum load (N_{max}), the load measured by the load cells on the control bar at peak load (N^*; where applicable), and the maximum load measured with zero load on the control bar load cell (called "free load", N_{free}) are listed. It should be noted that in most cases the load N^* is practically negligible.

#	Wall	Code	N_{max} (kN)	N^* (kN)	N_{free} (kN)
1	W0	1A-100-0.2-W0-1	17.78	-	17.78
	W0	1A-100-0.2-W0-2	23.68	-	23.68
	W0	1A-100-0.2-W0-3	19.86	-	19.86
	W0	1A-100-0.2-W0-4	18.99	-	18.99
	W1	1A-100-0.2-W1-5	22.43	-	22.43
	W3	1A-100-0.2-W3-6	13.18	-	13.18
	W3	1A-100-0.2-W3-7	12.24	-	12.24
	W3	1A-100-0.2-W3-8	13.92	-	13.92
2	W1	2A-100-0.2-W1-1	35.47	-	35.47
	W2	2A-100-0.2-W2-2	36.18	-	36.18
	W3	2A-100-0.2-W3-3*	25.91	1.49	23.96
3	W1	3A-100-0.2-W1-1	39.38	-	39.38
	W2	3A-100-0.2-W2-2*	48.64	0.00	48.64
	W3	3A-100-0.2-W3-3*	32.82	0.00	32.82
4	W1	4A-100-0.2-W1-1	62.57	-	62.57
	W2	4A-100-0.2-W2-2*	58.72	0.00	58.72
	W3	4A-100-0.2-W3-3*	40.10	0.00	40.10
	W3	4A-100-0.2-W3-4*	43.87	2.90	41.87
5	W1	5A-100-0.2-W1-1	53.76	-	53.76
	W2	5A-100-0.2-W2-2*	59.86	9.02	55.57
	W3	5A-100-0.2-W3-3*	51.73	10.66	48.90
	W3	5A-100-0.2-W3-4*	73.11	16.47	49.13

Table 1: Test results.

Reference tests on single anchors were executed according to the EAD [14] test procedure. The load-displacement curves and failure modes are shown in Figure 4 and Figure 5, respectively. It can be observed that in specimens W0 and W1, characterized by a mortar of higher strength, the failure mode was mixed cone and pull-out (involving also a part of the brick), while in specimen W3 the failure mode was anchor pull-out from the mortar bed joint (involving only a limited part of the brick). The same considerations can be made for the measured peak load (higher values for W0 and W1 compared to W3).

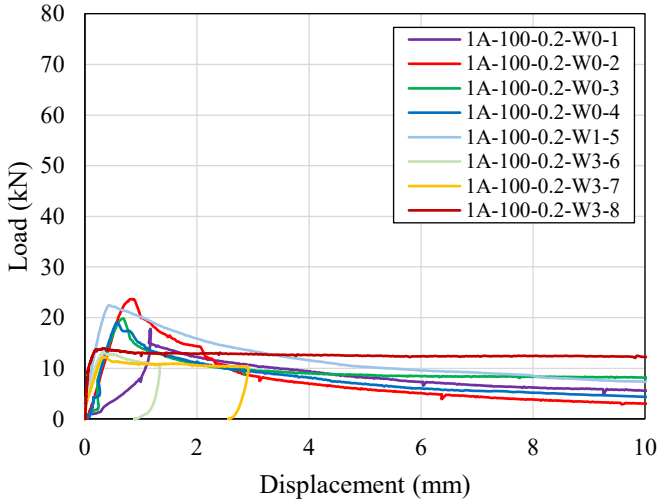

Figure 4: Load vs displacement curves for single (reference) anchor tests.

Figure 5: Failure modes for single anchor tests (left, 1A-100-0.2-W0-3; right, 1A-100-0.2-W3-7).

In the case of multiple anchors, if significant rotation of the baseplate was observed, tests were performed with the anti-rotation system. The load-displacement curves of these tests are presented in Figure 6. Again, the influence of the mortar strength can be appreciated (e.g. double anchor tests, W1-W2 vs. W3, Figure 6a or quadruple anchor tests, W1-W2 vs. W3, Figure 6c).

As the number of anchors increased, the volume of masonry involved in the failure mechanism increased as well, although the damage observed was rather limited (Figure 7). Specimens W0 and W1 show larger damaged volumes, while wall W3 shows less damage due to the lower strength of the mortar, except in the case of the 5 anchors test, where the influence of the mortar strength seems to be negligible.

The test results could be organized by grouping them as a function of the mortar strength of the wall and determining the mean values and the coefficient of variation of the maximum load to find possible relationships with the number of anchors. The average maximum load measured with the load cell (N_m) together with its coefficient of variation (cov,N_m) and the average maximum load measured with the loose control bars (N_{free}) with the corresponding coefficient of variation (cov,N_{free}) are listed in Table 2. Generally, the coefficients of variation of the free load cov,N_{free} are very low, except for the case of group of three anchors in high strength walls (W1, W2) where the cov,N_{free} was 14.9% due to the fact that test 3A-100-0.2-W1-1 showed a large rotation of the baseplate during the test (Figure 3). The same consideration can be made for

cov,Nm, except for the cases of 4 and 5 anchors, where the values are slightly higher than the corresponding ones of *cov,Nfree*.

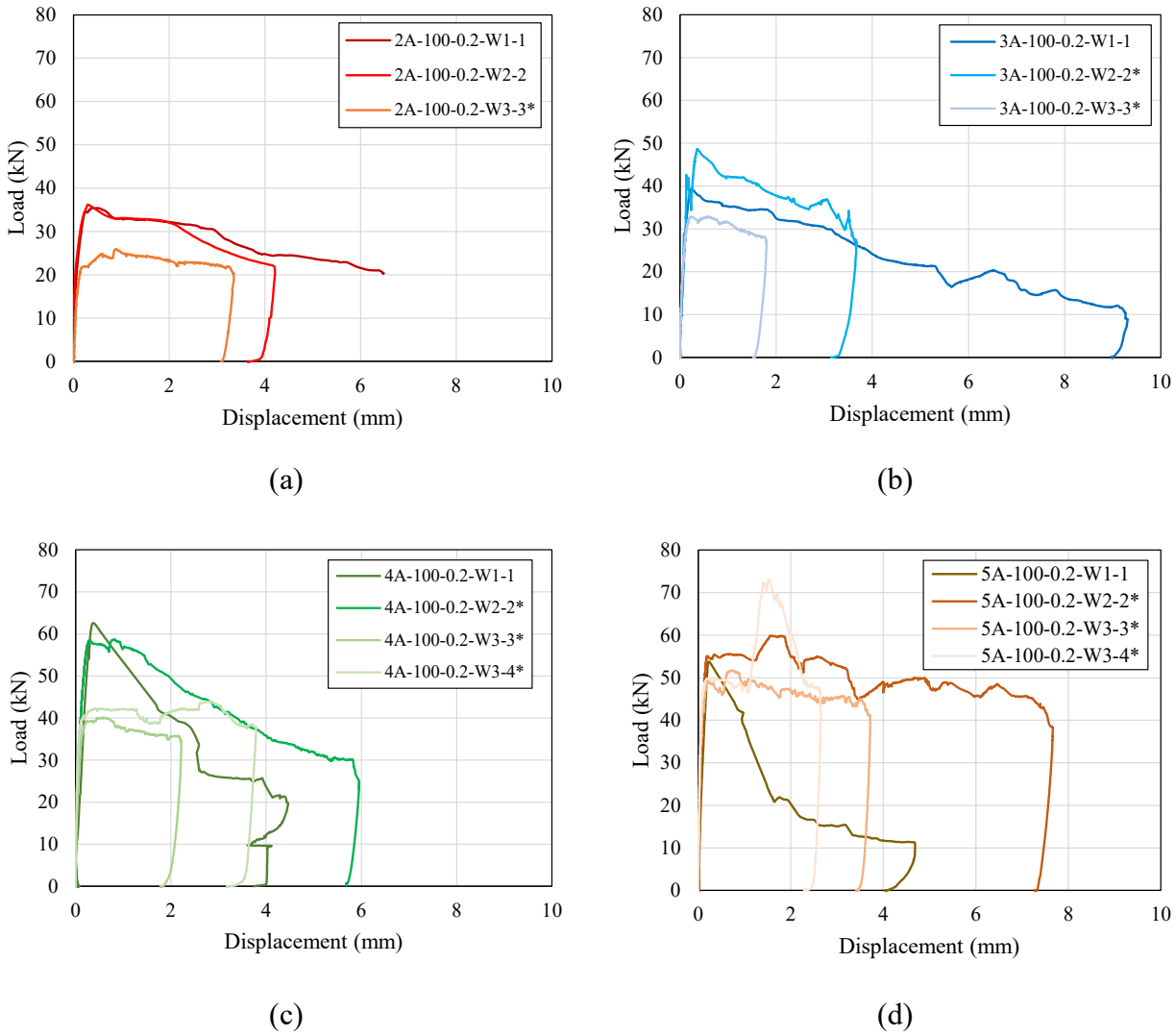

Figure 6: Load vs displacement curves for: (a) double, (b) triple, (c) quadruple, and (d) quintuple anchor tests.

# anchors	# of tests	Wall	N_m (kN)	cov,N_m	N_{free} (kN)	cov,N_{free}
1	5	W0-W1	20.55	11.9%	20.55	11.9%
1	3	W3	13.11	6.5%	13.11	6.5%
2	2	W1-W2	35.83	1.4%	35.83	1.4%
2	1	W3	25.91	-	23.96	-
3	2	W1-W2	44.01	14.9%	44.01	14.9%
3	1	W3	32.82	-	32.82	-
4	2	W1-W2	60.64	4.5%	60.64	4.5%
4	2	W3	41.99	6.3%	40.99	3.0%
5	2	W1-W2	56.81	7.6%	54.66	2.3%
5	2	W3	62.42	24.2%	49.02	0.3%

Table 2: Test results grouped by the mortar strength of the walls.

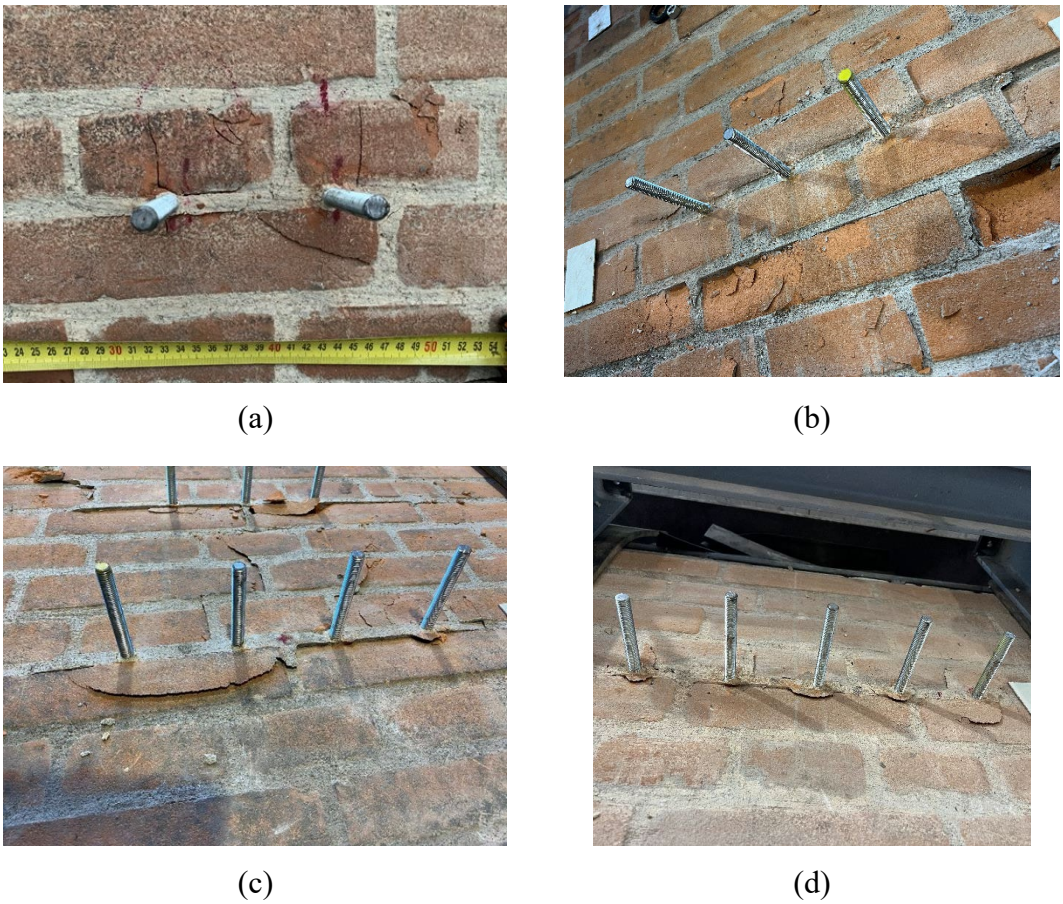

(a) (b)

(c) (d)

Figure 7: Failure modes for multiple anchor tests: (a) 2A-100-0.2-W3-3*, (b) 3A-100-0.2-W3-3*, (c) 4A-100-0.2-W2-2, and (d) 5A-100-0.2-W3-3*.

The maximum loads obtained from all tests can be plotted against the number of anchors to find possible relationships between them. Linear and quadratic trend-lines are presented in Figure 8 (left) showing good coefficients of determination even if the results are scattered. This can be explained by the fact that two types of walls are considered together (high and low strength mortar). To improve the quality of the prediction trend-lines, the results were divided into two groups depending on the mortar strength (W0-W2 and W3) of the wall, obtaining more meaningful and clearer trend-lines (Figure 8, right).

From Figure 8 (right) it can be seen that the maximum load of a five-anchor system is not greater than that of a four-anchor system, indicating that a sort of asymptotic value of the total capacity of the connection is reached in the case of high strength mortar specimens (W0-W2). For this reason, a quadratic trend-line seems to fit the results better than a linear one (dashed blue lines in Figure 8 right). On the contrary, for low strength mortar specimens (W3), the linear fit seems to be good (dashed red line in Figure 8 right).

A possible physical explanation for this behavior can be found by considering the volume of masonry involved in the failure of the connection. Given that the tested configuration considers a low spacing over embedment depth ratio ($s/h_{ef} = 1$), in case of high strength mortar specimens, the failure mechanism involved a large part of the wall in case of a high number of anchors, leading to a strong interaction between the anchors and consequently to a reduction of the total failure load. On the contrary, in the case of low strength mortar specimens, the failure mode of the connection shows smaller failure areas (pull-out failure instead of mixed cone and pull-out failure), leading to a situation where the interaction between the anchors is limited and thus to

a linear proportionality between the maximum capacity of the connection and the number of anchors.

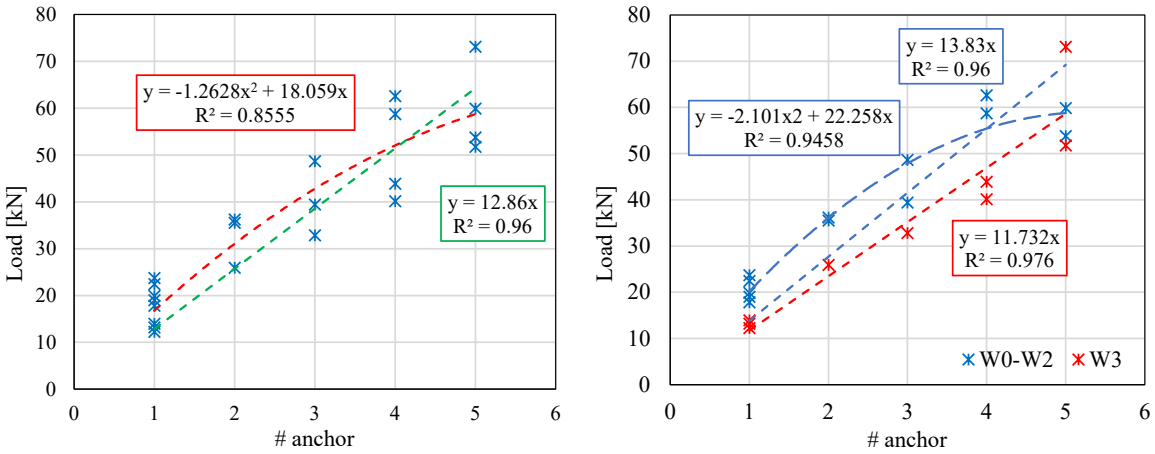

Figure 8: Maximum load vs number of anchors: ungrouped (left) and grouped (right) curves (red = low strength mortar; blue = high strength mortar).

4 NUMERICAL AND ANALYTICAL RESULTS

As the experimental results clearly showed, in linear fastening systems, the possible eccentricity and scattering of the failure load of the anchors could affect the overall capacity of the system. In order to better understand the influence of these phenomena on the behavior of the connection, a finite element of the linear fastening system was developed and some numerical analyses were performed.

The finite element (FE) model was implemented considering: (i) a stiff beam element to simulate the baseplate, (ii) nonlinear springs with a piecewise linear constitutive law modeling the anchor behavior in tension, and (iii) a pair of gap links at each end of the beam to model the contact between the baseplate and the masonry surface (active only in compression). A possible layout of the finite element model with 5 anchors is shown in Figure 9 (left).

To determine the idealized load-displacement curve of a single anchor in tension to be implemented in the finite element model, the experimental results obtained from the pull-out tests on single anchor installed in the high strength mortar specimen W0 were considered. The idealized piecewise linear load-displacement curve that fits the four experimental curves is represented in Figure 9 (right) together with the acquired curves.

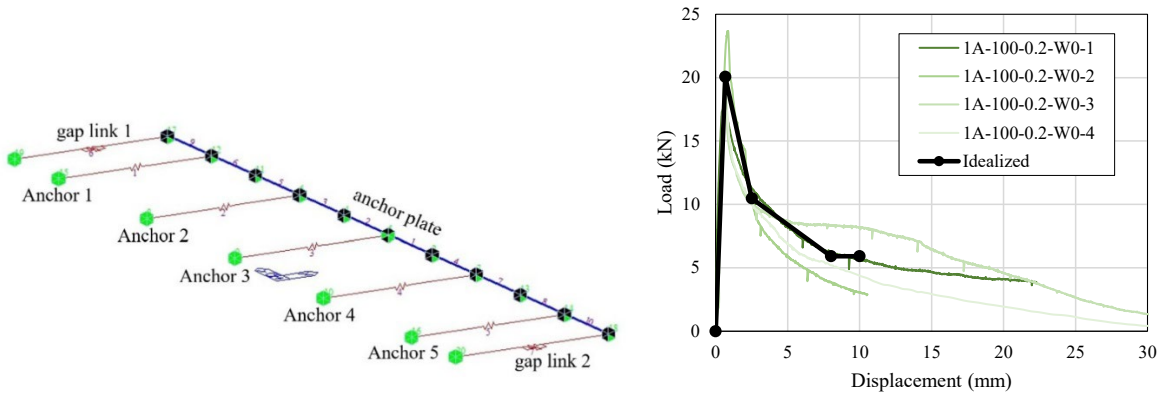

Figure 9: FE numerical model (left), experimental and idealized load-displacement curves (right).

The FE model gave the possibility to consider the influence of three different parameters on the overall capacity of the linear fastening system: (i) the eccentricity of the applied displacement; (ii) the scatter of the anchor pullout strength; and (iii) the group effect (interaction between anchors).

On the basis of the results of all the analyses, the overall capacity F_m of the linear fastening system can be expressed by the following relationship:

$$F_m = n \cdot \alpha_e(n,e) \cdot \alpha_{sc}(n) \cdot \alpha_i(n) \cdot f_{1,m} \quad (1)$$

where n is the number of anchors and $f_{1,m}$ (equal to 20.08 kN) is the mean maximum load of the four tests on a single anchor in W0 specimens.

The coefficient $\alpha_e(n,e)$ takes into account the influence of a possible small unintentional eccentricity e (in the range of 0 to 5% of the length L of the baseplate) on the overall capacity of the connection and can be expressed by:

$$\alpha_e(n,e) = 1 - k \cdot \frac{e}{L} \quad (2)$$

where the constant k has been determined by fitting the numerical results to the experimental curves (k = 1.87 for n = 1, k = 3.60 for n > 1). This coefficient, due to the combination of the eccentricity and the brittle behavior of the anchors, causes a reduction of the overall capacity F_m of the eccentrically loaded linear fastening system with respect to the symmetrical loading configuration.

The effect of the scatter of the maximum tensile load of a single anchor $f_{1,m}$ on the capacity of the linear fastening system can be described by the coefficient $\alpha_{sc}(n)$. The difference between the overall capacity of the system F_m with respect to the theoretical capacity of a perfectly centered load on a perfect system without any strength scatter ($F_{m,th} = n \cdot f_{1,m}$) can be described as a function of the number of anchors n by the following expression:

$$\alpha_{sc}(n) = 0.0055 \cdot n^2 - 0.0367 \cdot n + 1.0239 \quad (3)$$

obtained by fitting the results of the numerical analyses.

Finally, to take into account the possible interaction between the anchors loaded in tension, a coefficient $\alpha_i(n)$ is defined on the basis of the overlapping of their masonry outbreak cones [22], as follows:

$$\alpha_i(n) = \frac{l+(n-1)\cdot s}{n \cdot l} \quad (4)$$

where l is the side length of the pyramid modeling the outbreak cone and s is the spacing of the anchors. In this expression, the side length of the square base of the pyramid l was assumed to be equal to $2 \cdot h_{ef}$.

The proposed analytical model was then checked against the experimental results available for the high strength mortar specimens. For the comparison, the following input data were considered: $f_{1,m}$ = 17.76 kN, e = 0% or 1% of L, h_{ef} = 100 mm, s = 100 mm, l = 200 mm, L = 500 m. The comparison between the numerical predictions via Equation 1 (in case of symmetrical loading, $e = 0\% \cdot L$, or small eccentricity, $e = 1\% \cdot L$, as in the tests) and the experimental results is presented in Figure 10.

In general, the comparison between predicted capacity of the linear fastening system and experimental results shows a good agreement, while staying on the safe side. It can also be noted that the interaction between the anchors is the most influential parameter up to groups of 5 or 6 anchors, while beyond this number the interaction effect remains almost constant.

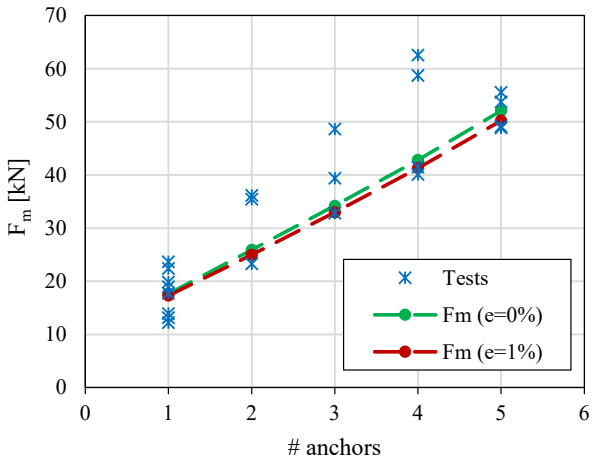

Figure 10: Numerical model vs experimental results.

5 CONCLUSIONS

Linear fastening is commonly used to connect slabs to walls in existing masonry structures. Existing design codes cover this type of application only up to two anchors per connection, but in most cases the number of anchors involved is greater than two.

This paper aims to improve the knowledge of the behavior of linear fastening systems through experimental and numerical considerations on different configurations of the connection, involving up to 5 in-line anchors. Finally, an analytical expression to predict the tensile capacity of the connection has been proposed and validated. The main findings of this research are:

- a linear relationship between the tensile capacity of the connection and the number of anchors has been obtained in walls with low strength mortar; this is probably due to the pull-out failure of the anchors, which results in limited damage to the masonry and a situation where there is no interaction between the anchors;
- on the other hand, for walls with high strength mortar, a non-linear relationship can be recognized, showing an asymptotic tensile capacity of the connection for a number of anchors greater than 4; in this case, the observed masonry damage is higher and the interaction between the anchors is greater;
- the numerical analyses showed that a small eccentricity of the applied displacement or the scatter of the anchor strength can lead to a reduction of the theoretical load capacity of the connection;
- the proposed tensile capacity prediction formula has been validated with the available experimental data, showing good agreement between numerical predictions and test results.

REFERENCES

1. Vlachakis, G.; Vlachaki, E.; Lourenço, P.B. Learning from Failure: Damage and Failure of Masonry Structures, after the 2017 Lesvos Earthquake (Greece). *Eng Fail Anal* **2020**, *117*, doi:10.1016/j.engfailanal.2020.104803.
2. Lourenço, P.B.; Mendes, N.; Ramos, L.F.; Oliveira, D. V. Analysis of Masonry Structures without Box Behavior. *International Journal of Architectural Heritage* **2011**, *5*, doi:10.1080/15583058.2010.528824.

3. Tselios, I.; Vintzileou, E.; Karagiannaki, D.; Christidis, K.; Palieraki, V.; Welz, G. Anchors to Solid Clay Brick Masonry in Tension: Behavior under Monotonic and Repeated Loading for Constant Embedment Depth. *Applied Sciences (Switzerland)* **2023**, *13*, doi:10.3390/app132312917.
4. Del Vecchio, C.; Maddaloni, G.; Pecce, M.R. Pull-out Tests on Injected Steel Anchors in a Masonry Tuff Wallet. In Proceedings of the Procedia Structural Integrity; 2022; Vol. 44.
5. Foraboschi, P. Shear Strength of the Anchor Embedded into Masonry. *Eng Struct* **2023**, *294*, doi:10.1016/j.engstruct.2023.116749.
6. Ceroni, F.; Darban, H.; Caterino, N.; Luciano, R. Efficiency of Injected Anchors in Masonry Elements: Evaluation of Pull-out Strength. *Constr Build Mater* **2021**, *267*, doi:10.1016/j.conbuildmat.2020.121707.
7. Burton, C.; Visintin, P.; Griffith, M.; Vaculik, J. Laboratory Investigation of Pull-out Capacity of Chemical Anchors in Individual New and Vintage Masonry Units under Quasi-Static, Cyclic and Impact Load. *Structures* **2021**, *34*, doi:10.1016/j.istruc.2021.08.016.
8. Paganoni, S.; D'Ayala, D. Testing and Design Procedure for Corner Connections of Masonry Heritage Buildings Strengthened by Metallic Grouted Anchors. *Eng Struct* **2014**, *70*, doi:10.1016/j.engstruct.2014.03.014.
9. Cattaneo, S.; Crespi, P.; Scamardo, M.; Vafa, N. Cyclic Behavior of Masonry Walls Retrofitted with Post-Installed Twisted Bars or Bonded Rebars. *Constr Build Mater* **2023**, *409*, 134026, doi:10.1016/j.conbuildmat.2023.134026.
10. Maddaloni, G.; Di Ludovico, M.; Balsamo, A.; Prota, A. Out-of-Plane Experimental Behaviour of T-Shaped Full Scale Masonry Wall Strengthened with Composite Connections. *Compos B Eng* **2016**, *93*, doi:10.1016/j.compositesb.2016.03.026.
11. Scamardo, M.; Cattaneo, S.; Crespi, P.; Vafa, N. Cyclic Behavior of C-Shaped Masonry Wall Retrofitted with Twisted Bars or Bonded Rebars. *Constr Build Mater* **2024**, *443*, 137703, doi:10.1016/j.conbuildmat.2024.137703.
12. Moreira, S.; Ramos, L.F.; Oliveira, D. V.; Lourenço, P.B. Experimental Behavior of Masonry Wall-to-Timber Elements Connections Strengthened with Injection Anchors. *Eng Struct* **2014**, *81*, doi:10.1016/j.engstruct.2014.09.034.
13. Longarini, N.; Crespi, P.; Scamardo, M. Numerical Approaches for Cross-Laminated Timber Roof Structure Optimization in Seismic Retrofitting of a Historical Masonry Church. *Bulletin of Earthquake Engineering* **2020**, *18*, 487–512, doi:10.1007/s10518-019-00661-w.
14. EOTA *EAD 330076-01-0604 Metal Injection Anchors for Use in Masonry*; 2021;
15. ASTM C67/C67M − 21 Standard Test Methods for Sampling and Testing Brick and Structural Clay Tile. *ASTM International* **2021**.
16. ASTM C1006-13 *Standard Test Method for Splitting Tensile Strength of Masonry Units*; 2013; Vol. 07;
17. American Society for Testing and Materials Astm C109/C109M. *Standard Test Method for Compressive Strength of Hydraulic Cement Mortars* **2021**, *04*.
18. ASTM International *ASTM C348-21 Standard Test Method for Flexural Strength of Hydraulic-Cement Mortars*; 2021;
19. ISO 898-1 Mechanical Properties of Fasteners Made of Carbon Steel and Alloy Steel —Part 1: Bolts, Screws and Studs with Specified Property Classes — Coarse Thread and Fine Pitch Thread. *Iso* **2009**, *2009*.
20. ETA-22/0395 *Injection System Hilti HIT-HY 270 in Solid Bricks. Metal Injection Anchors for Use in Masonry*; 2022;

21. Vintzileou, E.; Tselios, I.; Welz, G.; Arvanitis, C. Steel Anchors to Masonry – Double and Triple Anchors Installed in Line . In Proceedings of the 18th World Conference on Earthquake Engineering (WCEE2024); Milan, 2024.
22. CEN *EN1992-4 - Eurocode 2: Design of Concrete Structures - Part 4: Design of Fastenings for Use in Concrete*; 2018;